A Comparison of Creep Rupture Behaviour of 2.25Cr-1Mo And 9Cr-1Mo Steels and Their Weld Joints

K. Laha, K.S. Chandravathi, K. Bhanu Sankara Rao, S.L. Mannan and D.H. Sastry*

Materials Development Group, Indira Gandhi Centre for Atomic Research
Kalpakkam - 603 102, India
**Metallurgy Department, Indian Institute of Science*
Bangalore -560 012, India

(Received January 6, 1999)

ABSTRACT

Creep rupture behaviour of 2.25Cr-1Mo and 9Cr-1Mo base metals and weld joints has been studied at 823 K over a stress range of 100-250 MPa. In the stress range examined, 2.25Cr-1Mo steel showed better creep rupture strength compared to 9Cr-1Mo steel. Both the weld joints displayed a creep rupture strength inferior to those of their respective base metals. Failure occurred in the respective intercritical region of the heat affected zone (HAZ) in both the steel weld joints. At a given applied stress, the difference in rupture life of base and weld joint was more pronounced in 2.25Cr-1Mo steel than in 9Cr-1Mo steel and this difference increased with decrease in applied stress. As the presence of Mo_2C precipitate imparts creep resistance to 2.25Cr-1Mo steel, its absence in the intercritical HAZ region of the joint is held responsible for its poor creep life. On the other hand, 9Cr-1Mo steel which is strengthened by solid solution hardening and dislocation substructure, is less prone to degradation in the intercritical region. Also, the presence of δ-ferrite in the coarse grain region of HAZ of 9Cr-1Mo steel reduces its grain growth tendency and also its susceptibility to intergranular creep cavitation compared to 2.25Cr-1Mo steel.

1.0 INTRODUCTION

Cr-Mo ferritic steels are extensively used as structural materials in steam generating system of both nuclear as well as conventional power plants and also in chemical processing industries. Under creep conditions, the performance of weld joints of these alloys might be a life limiting factor /1-4/. In the design of welded components for high temperature applications, the allowable stress is often based on the creep rupture strength of the wrought material, while it is generally observed that the creep rupture strength of the weld joint is inferior to that of the base metal. A high percentage of service failures have been reported to occur in the microstructurally altered and inhomogeneous region of the base metal i.e. the HAZ in the weld joints /1,2,5,6/. The microstructural inhomogenity in the HAZ results from the complex thermal treatments to which this region is subjected to during welding.

This investigation is aimed at the understanding of microstructures developed across the weld joint and the consequent creep behaviour of similar joints of 2.25Cr-1Mo and 9Cr-1Mo steels. Creep rupture properties of both the weld joints have been compared and the differences attributed to different HAZ microstructures developed across the weld joints and their tensile properties determined from simulated HAZ structures.

2.0 EXPERIMENTAL DETAILS

Plates of 2.25Cr-1Mo as well as 9Cr-1Mo steel were welded by manual metal arc welding process using basic coated 2.25Cr-1Mo and 9Cr-1Mo electrodes respec-

Table-1
Chemical Composition (wt%)

Material	C	Si	Mn	P	S	Cr	Mo	Fe
2.25Cr-1Mo Base Metal	0.06	0.18	0.48	0.008	0.008	2.18	0.93	Bal
2.25Cr-1Mo Weld Metal	0.05	0.40	0.72	0.020	0.012	2.30	1.10	Bal
9Cr-1Mo Base Metal	0.10	0.49	0.46	0.008	0.002	8.36	0.93	Bal
9Cr-1Mo Weld Metal	0.12	0.52	0.52	0.003	0.030	8.90	0.98	Bal

tively. Details of the weld edge preparation and the welding conditions employed were reported earlier /1,2/. The chemical compositions of the base and weld metals for the two materials are listed in Table-1. The weld joints were examined by radiography for their soundness and were later subjected to a post weld heat treatment at 973 K for 60 minutes followed by air cooling.

Base metal and weld joint specimens of 5 mm diameter and 50 mm gauge length were machined from the weld pads. Creep tests were carried out at 823 K over a stress range of 100-250 MPa. The temperature was controlled within ±2 K over the entire gauge length. The creep elongation was measured continuously during the tests. All the tests were run to fracture.

Optical metallographic examination of the polished sections of both the weld joints was carried out in the as-welded, PWHTed and creep tested conditions. The etchants used were 2% Nital and Villela's reagent for 2.25Cr-1Mo and 9Cr-1Mo steel respectively. Vickers hardness measurements under a load of 50 grams were carried out on the weld joints of both the steels.

3.0 EXPERIMENTAL RESULTS

3.1 Microstructures

The microstructure of 2.25Cr-1Mo base metal in the normalized (1223 K for 17 min) and tempered (1003 K for 60 min) condition consisted of about 70% granular bainite and 30% proeutectiod ferrite (Fig-1a). The microstructure of 9Cr-1Mo base metal in the normalized

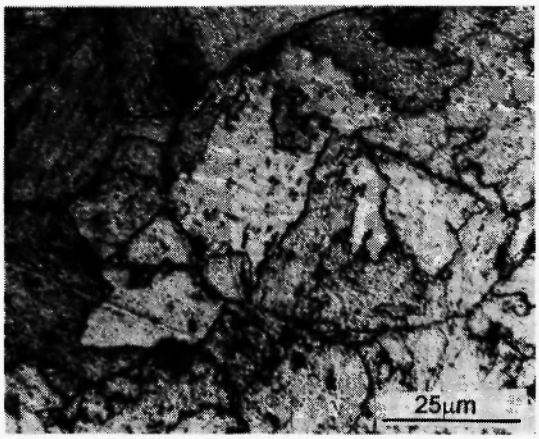

(a)

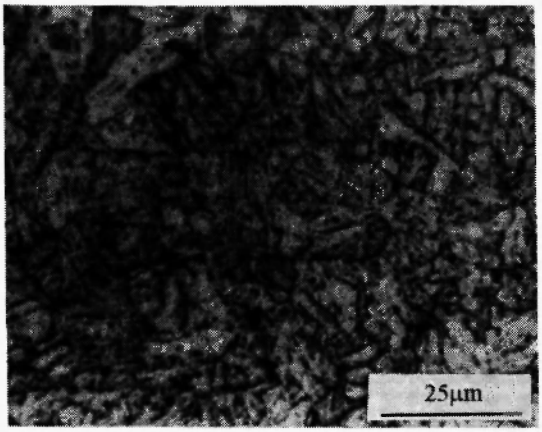

(b)

Fig. 1: Microstructures of (a) 2.25Cr-1Mo base metal (b) 9Cr-1Mo base metal.

(1223 K for 15 min) and tempered (1053 K for 120 min) condition exhibited tempered lath martensite (Fig-1b). In both the steels, the prior austenite grain boundaries as well as the lath boundaries (for 9Cr-1Mo) were decorated with precipitates.

The bulk of the weld metal microstructure in 2.25Cr-1Mo steel had a morphology characteristic of upper bainite and identifiable by its lath-like arrangement of ferrite (Fig-2a). Lath boundaries were decorated with carbides. Weld metal in 9Cr-1Mo steel (Fig-2b) was predominantly martensitic with stringers of δ-ferrite mostly along prior austenite grain boundaries and also between the martensitic laths.

The microstructure of the HAZ in 2.25Cr-1Mo steel consisted of coarse grain (≈ 120 μm) bainite (Fig-3a) near the fusion boundary followed by fine grain (~ 15 μm) bainite (Fig-3b) and intercritical region (Fig-3c)

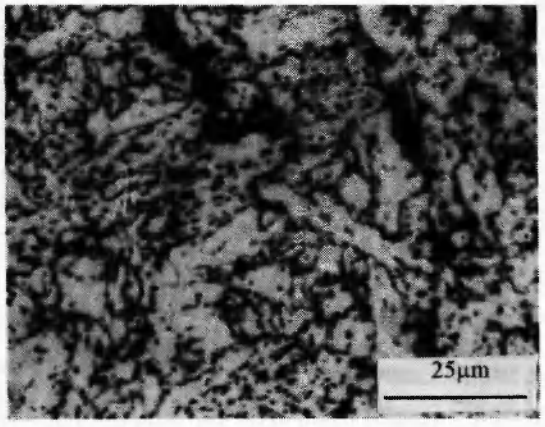

(a)

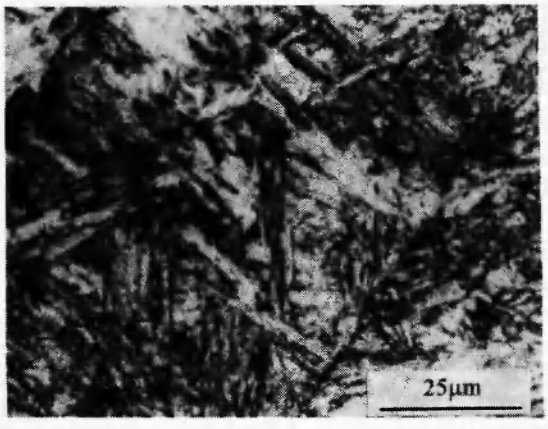

(b)

Fig. 2: Microstructures of (a) 2.25Cr-1Mo weld metal (b) 9Cr-1Mo weld metal.

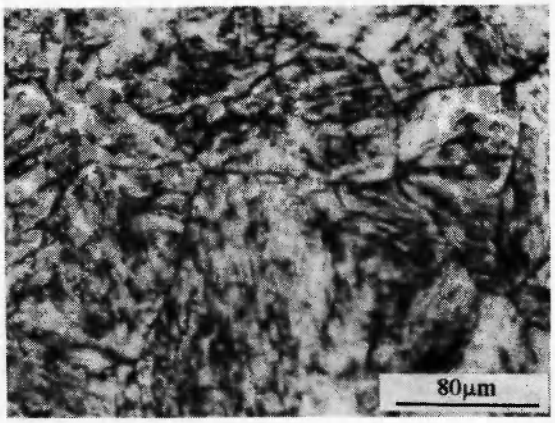

(a)

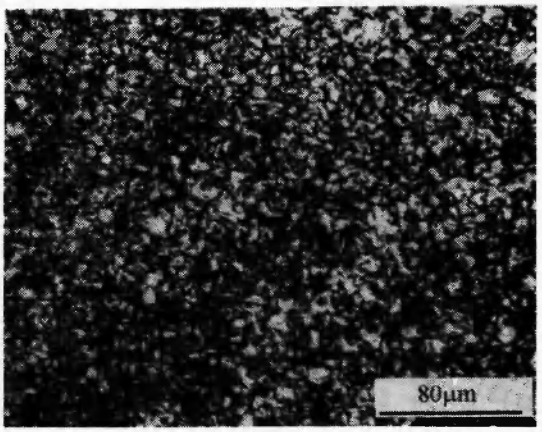

(b)

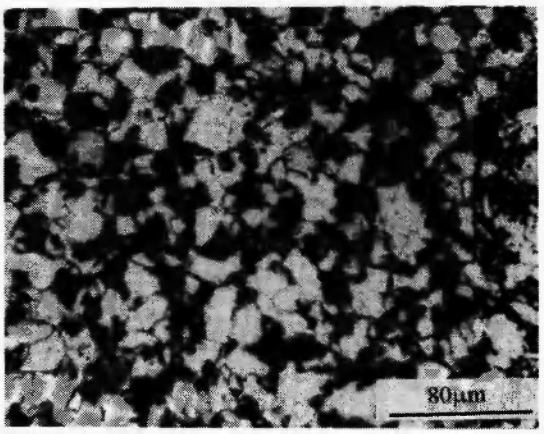

(c)

Fig. 3: Microstructures of HAZ of 2.25Cr-1Mo weld joint (a) coarse grain bainite (b) fine grain bainite (c) intercritical structure.

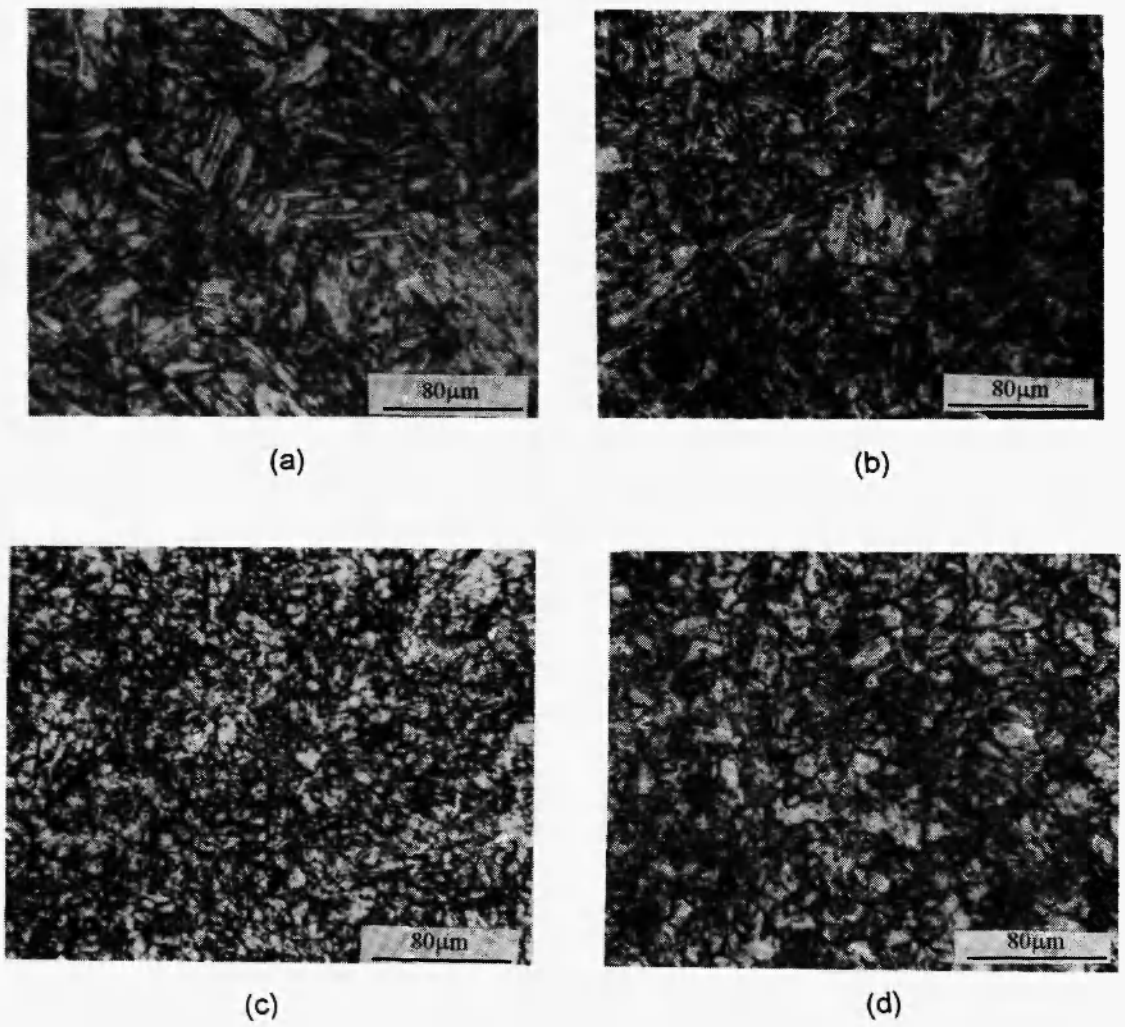

Fig. 4: Microstructures of HAZ of 9Cr-1Mo weld joint (a) coarse grain martensite with δ-ferrite (b) coarse grain martensite without δ-ferrite (c) fine grain martensite (d) intercritical structure.

adjacent to the affected base metal. The microstructure of 9Cr-1Mo HAZ revealed as coarse grain (≈80 μm) martensite with δ-ferrite mostly along the prior austenitic grain boundaries or between the martensitic laths (Fig-4a), coarse grain (≈ 60 μm) martensite without δ-ferrite (Fig-4b) followed by fine grain (≈ 15 μm) martensite (Fig-4c) and intercritical region (Fig-4d) adjacent to unaffected base metal.

3.2 Creep Results

Typical creep curves for the base metal and the weld joint at 150 MPa for both the steels are shown in Fig-5. Creep behaviour was well characterized by a small instantaneous strain on loading followed by well-defined primary, secondary and tertiary creep regions. Generally, weld joints exhibited relatively shorter primary and secondary stages of creep compared with their respective base metals.

The log-log variation of steady state creep rate ($\dot{\varepsilon}_s$) with applied stress (σ) for all the material conditions is shown in Fig-6. In all cases, the steady state creep data could be described by a power-law relation i.e. $\dot{\varepsilon}_s = A\sigma^n$, where n is the stress exponent and A is a material constant. In the stress range examined 2.25Cr-1Mo showed better creep strength than that of 9Cr-1Mo steel.

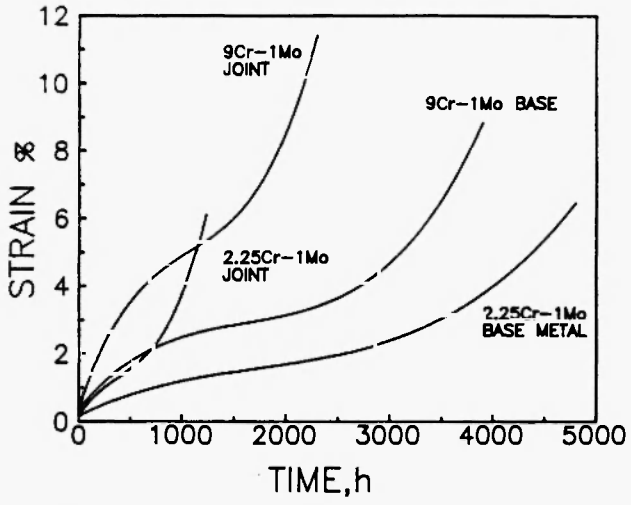

Fig. 5: Creep curves of base metals and weld joints of 2.25Cr-1Mo and 9Cr-1Mo steel at 823 K and 150 MPa.

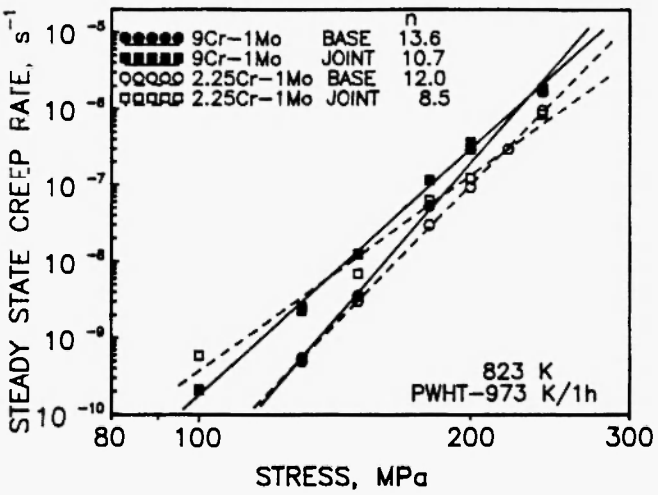

Fig. 6: Steady state creep rate as a function of applied stress of 2.25Cr-1Mo and 9Cr-1Mo base metals and weld joints.

The weld joint of both steels crept at a higher rate than their respective base metals.

The log-log variation of rupture life with applied stress for base and weld joint of the two steels is shown in Fig-7. 2.25Cr-1Mo base metal showed better rupture life than 9Cr-1Mo base metal in the stress range examined. The weld joint exhibited inferior rupture life compared to the base metal. The difference in the

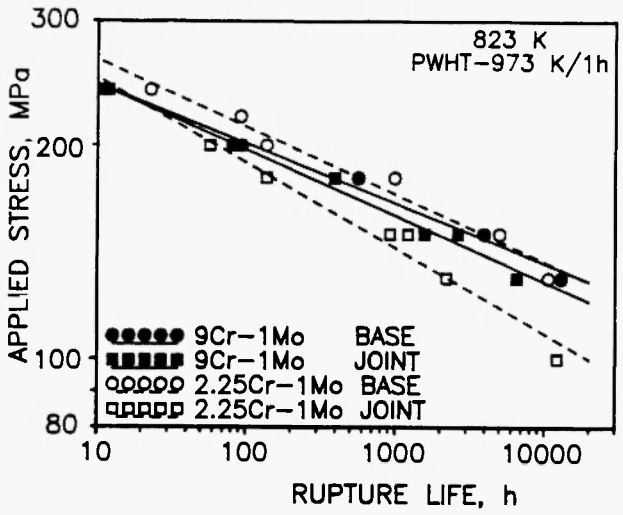

Fig. 7: Rupture life as a function of applied stress of 2.25Cr-1Mo and 9Cr-1Mo base metals and weld joints.

rupture life of base and weld joint increased with decrease in applied stress. Furthermore, this difference was more pronounced in the case of 2.25Cr-1Mo joint than in 9Cr-1Mo joint.

4.0 DISCUSSION

4.1 Microstructure

Granular bainite /7,8/ (Fig-1a) in 2.25Cr-1Mo base metal is believed to be present when the cooling rate during continuous cooling is comparatively low as in normalizing heat treatments. According to the precipitation sequence proposed by Baker and Nutting /9/, the precipitates expected at the end of tempering (1003 K for 60 minutes) and PWHT (973 K for 60 minutes) in 2.25Cr-1Mo base metal are Fe_3C and Mo_2C. Mo_2C precipitates uniformly in the matrix while Fe_3C precipitates mainly at grain boundaries. Fe_3C and Mo_2C are the only carbides that are reported to occur in the lath-like bainitic weld metal /10/.

The general sequence of carbide formation in 9Cr-1Mo base metal has been reported as /11/

$$Fe_3C \longrightarrow M_7C_3 \longrightarrow M_{23}C_6$$

M_2X type of carbide was also reported in the

intragranular region. The precipitates identified in normalized plus tempered 9Cr-1Mo steel were $M_{23}C_6$ at grain and lath boundaries while accicular Cr_2N precipitates were noticed in the intralath regions. Higher chromium content in 9Cr-1Mo coupled with higher cooling rate stabilized the high temperature phase δ-phase in the weld metal. Formation of δ-ferrite can promote secondary precipitation /12/.

The microstructures in the HAZ of weld joints (Figs-3 and 4) depend primarily on the peak temperature attained in the different regions during welding /1,6,13-15/. The region closest to the fusion boundary experiences peak temperature above Ac_4 (boundary between γ and γ + δ phase fields). Higher chromium content coupled with higher cooling rate stabilizes this δ-ferrite mostly along prior austenite grain boundaries in 9Cr-1Mo steel. The resulting structure near the fusion boundary after cooling is coarse grain martensitic with δ-ferrite along the prior austenite grain boundaries or between martensitic laths in 9Cr-1Mo steel (Fig-4a). On the other hand, HAZ near the fusion boundary is coarse grain bainite free of δ-ferrite in 2.25Cr-1Mo steel (Fig-3a). The presence of δ-ferrite in 9Cr-1Mo steel restricts the grain growth. Therefore, the grain size in the coarse grain region of HAZ was smaller in 9Cr-1Mo (≈ 80 μm) than in 2.25Cr-1Mo (≈120 μm). When the peak temperature attained is above Ac_3 but below Ac_4, the carbides which impede the austenite grain growth dissolve and hence coarse grain austenite would develop. On cooling this region transforms to a coarse grain martensite free of δ-ferrite in 9Cr-1Mo steel (Fig-4b). The grain size decreases with increasing distance from fusion boundary as the peak temperature experienced decreases, resulting in fine grain martensite in 9Cr-1Mo steel (Fig-4c) and fine grain bainite in 2.25Cr-1Mo steel (Fig-3b). When the peak temperature experienced is in the range between Ac_3 and Ac_1, only partial transformation to austenite takes place during heating. Consequently, the microstructure resulting on cooling would be a mixture of austenite transformation products surrounding the volumes of untransformed ferrite / bainite which has merely been tempered during thermal cycles (Figs-3c and 4d).

A very limited amount of information is available in literature regarding the types of carbide in HAZ of both the ferritic steels. Smith *et al* /16/ reported the absence of Mo_2C in the intercritical HAZ region of 2.25Cr-1Mo steel. Ray and Lauritzen /5/ have also not observed Mo_2C in the HAZ; they have reported M_7C_3, $M_{23}C_6$ and M_6C in the HAZ but did not clarify the specific zones in the HAZ. Several authors /17,18/ reported coarser carbides as well as equiaxed dislocation cells in the intercritically heat treated structure of 9Cr-1Mo steel compared with fine carbide and lath-martensite with high dislocation density in the base metal. Absence of Mo_2C in the intercritical region of HAZ in 2.25Cr-1Mo steel and coarser carbides and dislocation cells in the intercritical HAZ in 9Cr-1Mo are responsible for lower hardness observed in the intercritical HAZ region of both the steel weld joints (Figs-8 a and b). In these figures the hardness profiles across the joint after creep exposure (150 MPa, 823 K, rupture life 1215 and 2070

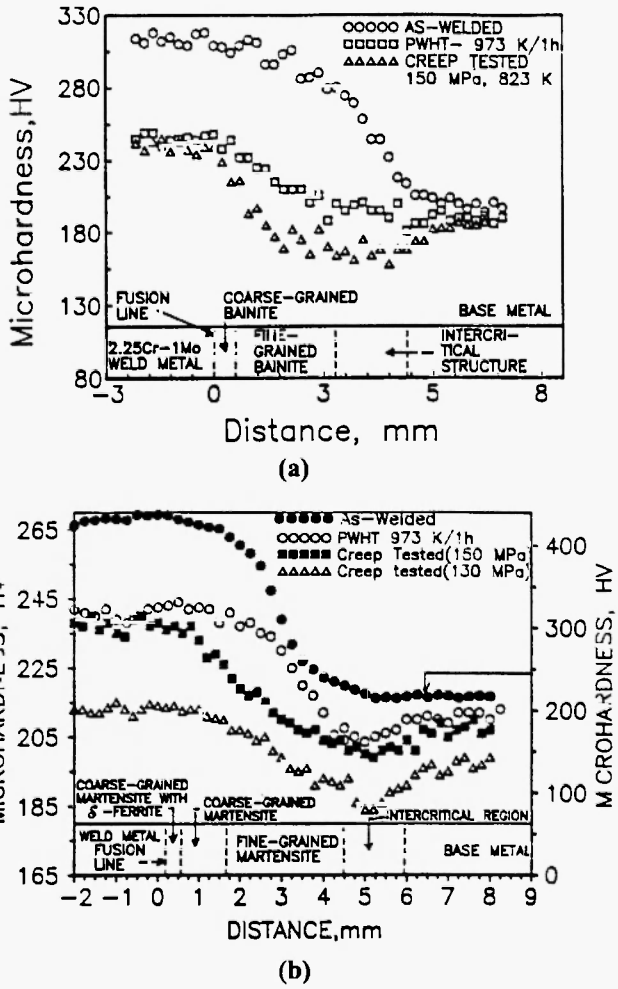

Fig. 8: Microhardness profile across weld joint (a) 2.25Cr-1Mo (b) 9Cr-1Mo steel.

hours respectively for 2.25Cr-1Mo and 9Cr-1Mo joint) are also shown. Creep exposure reduced the overall hardness of both the joints depicting the unstable nature of ferritic steel against creep exposure. However more noticeable is that the intercritical / fine grain HAZ in 2.25Cr-1Mo steel joint suffers a drastic reduction in hardness than that in 9Cr-1Mo weld joint.

4.2 Creep Behaviour

In the stress range investigated, 2.25Cr-1Mo steel base metal showed better creep rupture life compared to 9Cr-1Mo steel (Fig-7). This difference in the rupture lives decreased with decrease in stress and it is possible that at still lower applied stresses pertinent to service, 9Cr-1Mo steel might possess superior creep rupture life. Creep strength of 2.25Cr-1Mo steel has been attributed to the intragranular accicular Mo_2C particles /8,9/. Replacement of Mo_2C carbide by higher order coarser carbides leads to degradation of creep strength at lower applied stress in 2.25Cr-1Mo steel. On the other hand, 9Cr-1Mo steel owes its creep strength to finer martensitic laths with high dislocation density and interaction solid solution strengthening /18/. This should be maintained over longer duration of exposure.

Creep rupture lives of weld joint specimens were inferior to those of base metals in both the steels. Microstructural examination of the failed weld joint specimens of both the steel joints indicates that fracture occurred in the intercritical region of HAZ. In order to investigate as to how deformation proceeds across the gauge length of the weld joint during creep test and also to identify the specific region of the HAZ causing creep failure, an interrupted creep test was conducted and the strain distribution across the gauge length of the weld joint specimen was determined. The strain in the different zones of the weld specimen was determined at certain intervals of time by interrupting the test and measuring the distance between equally spaced Vickers' hardness indentations made on the specimen surface before the creep test. Creep strain distribution studies on both the ferritic steel weld joints at 823 K employing a stress of 150 MPa (Fig-9) clearly established that the creep strain became progressively localized within the intercritical region of HAZ as the creep test progressed, indicating that the intercritical structure is the weakest of all in the HAZ. The local strain accumulation in the intercritical region was also reflected in the faster creep rate of weld joint specimens (Fig-6). Comparing the strain distribution profiles of 2.25Cr-1Mo weld joint with those of 9Cr-1Mo weld joint it is evident that creep deformation was relatively more uniform across the gauge length for longer creep exposure time in 9Cr-1Mo steel than that in 2.25Cr-1Mo steel. This indicates that the microstructural degradation in 9Cr-1Mo ferritic steel due to thermal exposure (during welding thermal cycle) and creep exposure is less compared to that in 2.25Cr-1Mo ferritic steel.

In an attempt to assess the strength in the different constituents in HAZ of both the steels, these constituents were simulated by isothermal heat treatments /13,15/. The heat treatment cycles employed were based on the comparative evaluation of prior austenitic grain size, microconstituents and hardness of the heat treated samples with those of actual weld joints. Tensile tests /13,15/ conducted on the base metal and simulated HAZ structures of both the steels showed lower strength of the intercritically heated specimens (Figs-10 a and b). Poorer rupture life of weld joint of 9Cr-1Mo steel compared to base metal arised due to coarser carbides and equiaxed dislocation cell substructure in the intercritical region of the HAZ /16/. This is in contrast to fine carbides and lath-martensite with high dislocation density observed in the 9Cr-1Mo base metal /17,18/. Failure in intercritical HAZ region in 2.25Cr-1Mo steel could be attributed to the poor strength of this region due to the absence of Mo_2C carbide /5,16/.

At a given applied stress, the difference in the rupture life of the base metal and weld joint was more pronounced in 2.25Cr-1Mo steel than in 9Cr-1Mo steel and this difference increase with decrease in applied stress (Fig-7). Larger differences in tensile strength between base metal and simulated intercritical structure of HAZ in 2.25Cr-1Mo steel compared to those in 9Cr-1Mo steel are evident from Figs-10 a and b. This arose due to the difference in the nature of hardening in these two steels. Replacement of fine accicular intragranular Mo_2C particle by higher order, less effective carbides and their coarsening due to intercritical heat treatment and prolonged high temperature exposure would lead to pronounced

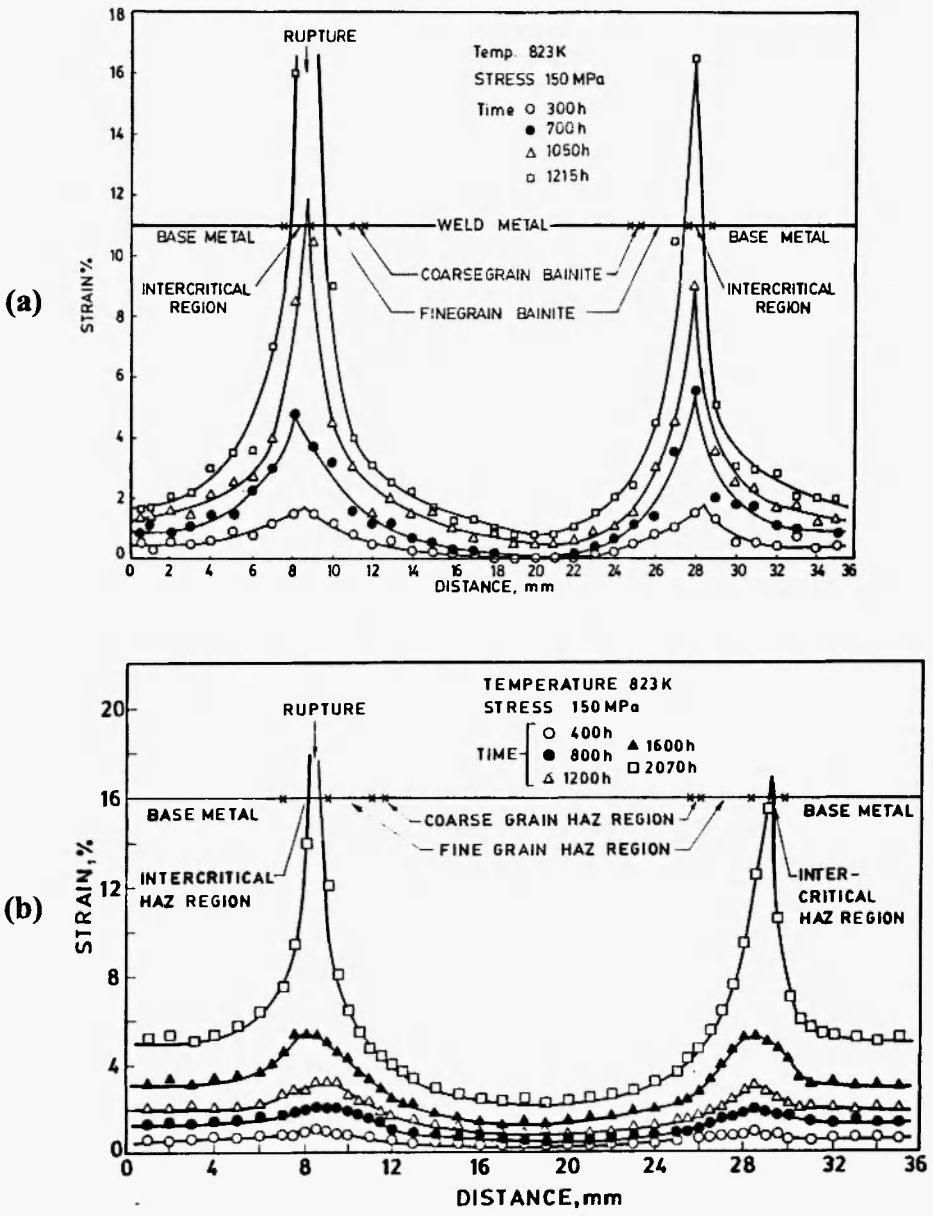

Fig. 9: Creep strain profile along the weld joint during creep testing (150 MPa and 823 K) (a) 2.25Cr-1Mo steel (b) 9Cr-1Mo steel.

degradation in strength in 2.25Cr-1Mo steel. However, in 9Cr-1Mo steel, the strengthening resulting from substructure and solid solution hardening appears to decline slowly under intercritical heat treatment and prolonged high temperature exposure /17,18/. Earlier studies have also indicated the stability of mechanical properties of 9Cr-1Mo steel when subjected to different heat treatments [/9/.

At lower applied stresses, even though failure occurred in the intercritical region of HAZ in 2.25Cr-1Mo steel weld joint, pronounced intergranular creep cavitation was observed in the coarse grain region of HAZ /2/. These observations indicated that if proper care is not taken during welding to refine the coarse grain of HAZ, such regions could be a possible site of failure. But no such creep cavitation was observed in the coarse grain HAZ of 9Cr-1Mo steel weld joint. Reduction in area in tensile tests of different HAZ

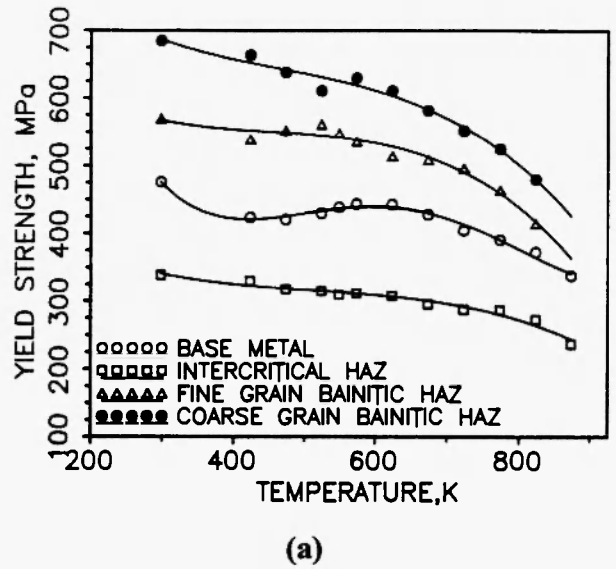

Fig. 10: Variation of tensile yield strength (0.2% off-set) with test temperature of base metal and simulated HAZ structures of (a) 2.25Cr-1Mo steel (b) 9Cr-1Mo steel.

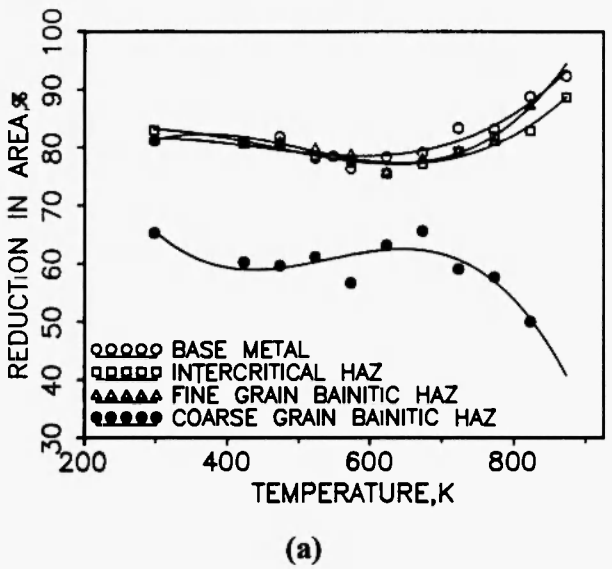

Fig. 11: Variation of tensile reduction in area with test temperature of base metal and simulated HAZ structures of (a) 2.25Cr-1Mo steel (b) 9Cr-1Mo steel.

structures and base metals in both the steels /11,15/ (Figs 11 a and b) showed a severe reduction of ductility value for coarse grain HAZ structure in 2.25Cr-1Mo steel compared to its base metal. By contrast, no such reduction was observed in the coarse grain HAZ region in 9Cr-1Mo steel. The presence of δ-ferrite along the prior austenite grain boundaries inhibited grain growth in comparison to 2.25Cr-1Mo steel and this soft phase reduced the susceptibility of the coarse grain region to intergranular cavitation. However, possible transformation of δ-ferrite after prolonged service condition into brittle intermetallics in 9Cr-1Mo steel might have a deleterious effect on creep strength and toughness, particularly in steels containing Nb, Ti, W /20/.

5.0 CONCLUSIONS

1) Weld joints of both the 2.25Cr-1Mo and 9Cr-1Mo steels showed inferior creep rupture lives compared to their respective base metals.
2) At a given applied stress, the difference in rupture life of base metal and weld joint was more pronounced for 2.25Cr-1Mo steel than for 9Cr-1Mo steel and this difference increased with decrease in applied stress.
3) Poor creep strengths in weld joints had been attributed to the microstructural degradation in the intercritical region of HAZ in both the steels.
4) The presence of soft δ-ferrite in the coarse grain region of HAZ in 9Cr-1Mo weld joint, restricted grain growth and reduced its susceptibility to intergranular creep cavitation compared to coarse grain region of 2.25Cr-1Mo weld joint.

6.0 ACKNOWLEDGMENTS

The authors express their deep sense of gratitude to Dr. Placid Rodriguez, Director, IGCAR, Kalpakkam and Dr. Baldev Raj, Director, MMG, IGCAR, Kalpakkam for their keen interest in this work and encouragement.

REFERENCES

1. K. Laha, K. Bhanu Sankara Rao and S.L. Mannan; *Mater. Sci. Engng.*, **A129,** 183 (1990).
2. K. Laha, K. Bhanu Sankara Rao and S.L. Mannan; in *Proc. Intl. Conf. on Creep of Materials*, Lake Buena Vista, Florida, USA, ASM, 1992; p.399.
3. W. Arnswald, R. Blum, B. Neubauer and P.E. Poulse; in *Proc. Intl. Conf. on Creep of Materials,* Tokyo, Japan, ASM, 1986; p. 367.
4. T.L. da Silveira and I. Le May; in *Proc. Intl. Conf. on Creep of Materials*, Lake Buena Vista, USA, ASM, 1992; p. 235.
5. P. Ray and T. Lauritzen; *Welding J.Res.Suppl.*, **65,** 45s (1986).
6. I.J. Chilton, A.T. Price and B. Wilshire; *Met. Technol.*, **11**, 383 (1984).
7. O.V. Serrano, G.R. Edwards and R.H. Frost; in *ASTM Spec.Tech.Publ.*, **755**, 275 (1982).
8. M.C. Murphy and G.D. Branch; *J. Iron Steel Inst.* **192**, 257 (1957).
9. R.G. Baker and J. Nutting; *J. Iron Steel Inst.*, **192**, 257 (1959).
10. C.D. Lundin, S.C. Kelly, R. Menon and B.J. Kruse; *Welding Research Council Bulletin*, **314**, 1 (1984).
11. J.M. Vitek and R.H. Klueh; *Met. Trans. A*, **149**, 1047 (1983).
12. F.B. Pickering and A.D. Vassiliou; *Met. Technol.*, 7, 409 (1980).
13. K. Laha, K. Bhanu Sankara Rao, K.S. Chandravathi and S.L. Mannan; *Trans. Indian Inst. Met.*, **46**, 77 (1993).
14. E.F. Nippes; *Welding J. Res. Suppl.*, **38**, 1s (1959).
15. K. Laha, K.S. Chadravathi, K.B.S. Rao and S.L. Mannan; *J. Pres. Ves.Piping*, **62**, 303 (1995).
16. E. Smith, B.E. Blanchard and R.L. Apps; in *Proc. Conf. on Welding of Creep Resistant Steels,* Cambridge, The Welding Institute, 1970; p. 79.
17. F. Arav, H.J. Jentferink, C.F. Etienne and J.C. Van Wortel; in *Proc. Intl. Conf. on Creep of Materials,* Lake Buena Vista, Florida, USA, ASM, 1992; p. 177.
18. W.B. Jones; in *Ferritic Steels for High Temperature Applications* (ed. Ashok K. Khare), American Society of Metals, 1983; p. 211.
19. B.J. Cane and R.S. Fidler; in *Proc. Intl. Conf. on Ferritic Steels for Fast Reactor Steam Generators,* London, BNES, 1978; p. 193.
20. R.S. Fidler and D.J. Gooch; in *Proc. Ferritic Steels for Fast Reactor Steam Generators*, London, BNES, 1978; p. 128.